

# Coupled circularly polarized electromagnetic soliton states in magnetized plasmas

G.P. Veldes,<sup>1</sup> N. Lazarides,<sup>2</sup> D.J. Frantzeskakis,<sup>3</sup> and I. Kourakis<sup>2,4,5,6</sup>

<sup>1</sup>*Department of Physics, University of Thessaly, Lamia 35100, Greece*

<sup>2</sup>*Department of Mathematics, Khalifa University, Abu Dhabi, United Arab Emirates*

<sup>3</sup>*Department of Physics, University of Athens, Panepistimiopolis, Zografos, Athens 15784, Greece*

<sup>4</sup>*Space & Planetary Science Center, Khalifa University, Abu Dhabi, United Arab Emirates*

<sup>5</sup>*Visiting Researcher, Department of Physics, University of Athens,*

*Panepistimiopolis, Zografos, Athens 15784, Greece*

<sup>6</sup>*Adjunct Researcher, Hellenic Space Center, Leoforos Kifissias 178, Chalandri, GR-15231 Athens, Greece*

The interaction between two co-propagating electromagnetic pulses in a magnetized plasma is considered, from first principles, relying on a fluid-Maxwell model. Two circularly polarized wavepackets by same group velocities are considered, characterized by opposite circular polarization, to be identified as left-hand- or right hand circularly polarized (i.e. LCP or RCP, respectively). A multiscale perturbative technique is adopted, leading to a pair of coupled nonlinear Schrödinger-type (NLS) equations for the modulated amplitudes of the respective vector potentials associated with the two pulses. Systematic analysis reveals the existence, in certain frequency bands, of three different types of vector soliton modes: an LCP-bright/RCP-bright coupled soliton pair state, an LCP-bright/RCP-dark soliton pair, and an LCP-dark/RCP-bright soliton pair. The value of the magnetic field plays a critical role since it determines the type of vector solitons that may occur in certain frequency bands and, on the other hand, it affects the width of those frequency bands that are characterized by a specific type of vector soliton (type). The magnetic field (strength) thus arises as an order parameter, affecting the existence conditions of each type of solution (in the form of an envelope soliton pair). An exhaustive parametric investigation is presented in terms of frequency bands and in a wide range of magnetic field (strength) values, leading to results that may be applicable in beam-plasma interaction scenarios as well as in space plasmas and in the ionosphere.

## I. INTRODUCTION

Electromagnetic (EM) pulse propagation in a plasma has been in the focus of researchers for decades. From a basic theoretical point of view, it is associated with fundamental physical processes involving various nonlinear mechanisms and instabilities, which have been attracting increasing interest since the early days of plasma research. Thanks to a series of seminal early studies [1–4] which set the foundations of contemporary laser-plasma interaction science [5, 6], the study of electromagnetic pulse propagation has been shown to be relevant with phenomena like parametric instabilities [7, 8], harmonic generation [9], self-focusing [10], intense electric and magnetic field [11, 12], and wakefield [13, 14] generation, among others. As laser power and technological sophistication increased, in the last decades, new regimes were attained where ultrashort ultrastrong electromagnetic (laser) pulses could be realized in the laboratory, thus entering the realm of relativistic dynamics (where the electron quiver velocity is comparable to the speed of light) [15] and, more recently, even quantum-electrodynamics [16–19]. EM beam propagation is nowadays a cutting edge topic in science, due to its relevance with applications including laser-assisted (inertial confinement fusion, ICF) schemes for energy production, to ion acceleration [20] and to sophisticated experimental diagnostic techniques [21] and thus one of the hottest topics in contemporary research.

The propagation of relativistic soliton pulses, which is our focus here, has not only been predicted by analytical

theory [1–4, 22, 31] and computer simulations [23–30], but also observed in laser-plasma interaction (LPI) experiments [32–39]. These are essentially electromagnetic pulses trapped in a plasma density cavitation with overdense boundaries [40–42]. As shown in Refs. 25 and 26, a big portion of the laser pulse (electromagnetic) energy becomes localized into a train of soliton-like structures, which may play a crucial role in laser-matter and laser-plasma interaction processes.

The generation of relativistic electromagnetic solitons is governed by various physical mechanisms, including dispersion due to the finite electron inertia and nonlinearity due to a relativistic electron mass variation as well as to ponderomotive forces. Various analytical studies have focused on elucidating the properties of relativistic EM solitons, most of them focusing on a one-dimensional (1D) relativistic fluid model comprising of coupled nonlinear equations for the vector and scalar potentials, coupled to the plasma. Circularly polarized (CP) EM solitons in a cold plasma were investigated early on by Kozlov *et al* [2], who relied on a quasineutrality hypothesis to establish the occurrence of small-amplitude localized solutions (solitary waves). Later, computer simulations have shed some light on large-amplitude (relativistic) pulses, wherein charge separation in the plasma may be significant [2]. Drifting envelope solitons of CP light were later modeled by Kaw and coworkers [3]. A stationary (zero group velocity) relativistic EM soliton solution with was shown to exist within a 1D cold plasma model in Ref. 4. Further remarkable works on 1D solitary waves in cold plasmas based on a perturbation technique include the studies by Kuehl and Zhang [43] and by Fa-

rina *et al* [42, 44], who incorporated the effect of ion motion in a fluid-Maxwell description. Later, Poornakala *et al* [45] discussed the existence of bright or dark type envelope solitons and identified associated regions in parameter space. Thermal effects were taken into account in Refs. 47 and 48. Single peak and multi-peak structures and their stability and mutual interaction properties were studied by Saxena *et al*, considering a non-uniform plasma [46], and also later in Refs. 49 and 50. Note, for rigor, that the aforementioned studies have focused on non-magnetized plasma.

Magnetization during laser plasma interactions has attracted significant attention, as it impacts both the laser pulse dynamics and the substrate i.e. the background plasma properties. Inertial confinement fusion (ICF) has triggered interest in the study of magnetized plasma-laser interaction [51, 52]. Experimental observations have confirmed the generation of intense magnetic fields (up to hundreds of MG) [12, 53–55] during LPI.

As regards EM pulse propagation in magnetized plasma, Shukla and Stenflo [56] studied stationary solitary wave electromagnetic field structures adopting a slowly varying envelope approximation, followed by Nagesha *et al* [57], who adopted a slowly varying envelop approximation and neglected perturbations in the longitudinal component of the electron momentum, to find stationary solutions for CP EM waves in cold magnetized plasma. Weakly super-acoustic (supersonic) EM envelope waves were studied by Rao [58]. The occurrence of standing 1D relativistic solitons in cold magnetized plasmas and the magnetic field's role on soliton stability was discussed by Farina *et al* [59], who found that the frequency interval for stable solitons depends on both the magnitude and the orientation of the magnetic field in a significant manner. Furthermore, the maximum field amplitude of the solitonic pulses essentially depends on the ambient magnetic field (strength).

In the article at hand, we have undertaken an analytical and numerical study of the interaction between left- and right-hand circularly polarized solitons in magnetized plasmas. Based on a fluid-Maxwell model, as starting point, we have established a system of scalar equations governing the propagation of circularly polarized EM waves in magnetized plasma. First, analysis of the linear regime has shown that, in certain frequency bands, left-hand circularly polarized (LCP-) and right-hand circularly polarized (RCP-) modes can propagate at the same group velocity. Next, we adopt a large-amplitude (nonlinear) approach, treating the model equations within an asymptotic multiscale expansion method. Assuming the existence of coupled localized (soliton) states for the magnetic vector potential, the analysis leads to a system of two coupled nonlinear Schrödinger (NLS) type equations for the respective EM field envelopes, i.e. for the right-hand circularly polarized (RCP-) and the left-hand circularly polarized (LCP-) mode respectively. The analysis of the coupled NLS equations shows that there are three types coupled (vec-

tor) solitons for certain frequency bands, namely,

- (a) a RCP-propagating bright soliton coupled with a LCP-propagating bright soliton,
- (b) a RCP-propagating bright soliton coupled with a LCP-propagating dark soliton, and
- (c) a RCP-propagating dark soliton coupled with a LCP-propagating bright soliton.

This paper is organized as follows. In Section II, we introduce the fluid-Maxwell model for magnetized plasma and discuss the underlying physics. In Section III, the system is linearized and the dispersive modes obtained are identified. In Section IV, we assume a coupled-mode solution, and apply a multiscale perturbative technique to derive a system of (two) coupled NLS equations for the respective wavepacket amplitudes. In Section V, we present analytical results for each type of vector soliton. Finally, in the concluding Section VI, we summarize our results.

## II. FLUID-MAXWELL MODEL FOR EM WAVES

We consider an electron-ion plasma, permeated by a uniform magnetic field along  $\hat{x}$ . The instantaneous state of the plasma is given by a number of dynamical state variables, namely: the electron number density  $n$ , fluid speed  $\mathbf{u} = u \hat{x}$  and momentum (vector)  $\mathbf{p} = (p_y, p_z)$ . These are subject to the influence of the electrostatic (scalar) potential  $\phi$  and the magnetic (vector) potential  $\mathbf{A} = (A_y, A_z)$ . All of these variables are functions of space  $x$  and time  $t$ , where one-dimensional (1D) propagation was considered, in the direction parallel to the magnetic field, i.e. along  $\hat{x}$ . Given the (high) frequency of interest, the ions will be assumed to be stationary.

Our analysis will be based on the following closed system of scalar equations which govern the propagation of the circularly polarized EM waves in magnetized plasma:

$$\frac{\partial^2 A_y}{\partial x^2} - \frac{\partial^2 A_y}{\partial t^2} = \frac{n}{\gamma} p_y, \quad (1)$$

$$\frac{\partial^2 A_z}{\partial x^2} - \frac{\partial^2 A_z}{\partial t^2} = \frac{n}{\gamma} p_z, \quad (2)$$

$$\frac{\partial}{\partial t}(p_y - A_y) + u \frac{\partial}{\partial x}(p_y - A_y) = -\frac{\Omega p_z}{\gamma} \quad (3)$$

$$\frac{\partial}{\partial t}(p_z - A_z) + u \frac{\partial}{\partial x}(p_z - A_z) = \frac{\Omega p_y}{\gamma} \quad (4)$$

$$\frac{\partial n}{\partial t} + \frac{\partial(nu)}{\partial x} = 0, \quad (5)$$

$$\frac{\partial(\gamma u)}{\partial t} = \frac{\partial}{\partial x}(\phi - \gamma) + \frac{1}{\gamma} \left[ p_y \frac{\partial}{\partial x}(p_y - A_y) + p_z \frac{\partial}{\partial x}(p_z - A_z) \right] \quad (6)$$

$$\frac{\partial^2 \phi}{\partial x^2} = n - 1. \quad (7)$$

All physical quantities have been normalized by appropriate scales, namely: the scalar and vector potentials are

normalized by  $mc^2/e$ , the electric field  $\mathbf{E}$  by  $m\omega_{pe}/e$ , the magnetic field by  $\mathbf{B}$  by  $m\omega_{pe}/e$ , the momentum by  $mc$ , the density by the  $n_0$ , the electron velocity by the light velocity  $c$ . Thus, in this framework the length is measured in units of the skin length  $c/\omega_{p0}$ , and time is measured in units of the plasma period (inverse plasma frequency)  $(\omega_{pe}^{-1})$ , where  $\omega_{pe} = \sqrt{4\pi n_0 e^2/m_e}$  (here  $n_0$  denotes the equilibrium electron density). Also, the electron momentum can be expressed as ,

$$\mathbf{P} = \mathbf{p}(x, t) + \gamma u(x, t)\hat{x} \quad (8)$$

for a circularly polarized EM pulse, where  $\gamma$  is the relativistic factor and we have used the notation  $\alpha = +1$  ( $\alpha = -1$ ) for left- (right-) hand circularly polarized electromagnetic waves.

### III. MULTIPLE SCALE ANALYSIS FOR A SINGLE CIRCULARLY POLARIZED MONOCHROMATIC WAVEPACKET

Let the state vector  $\mathbf{S} = (n, u, \phi; A_y, A_z; p_y, p_z)$  describe the state of the system at a given position  $x$  and time  $t$ . Assuming a moderate (but finite) deviation from the equilibrium state  $S^{(0)} = (1, 0, 0; 0, 0; 0, 0)$ , one may adopt a multiple scales perturbation technique by expanding the system's state as a series in terms of powers of a small parameter  $\epsilon \ll 1$  and subsequently considering multiharmonic analysis in each order. The method was described exhaustively in the past, e.g. in Ref. 60 in general, and also, for electrostatic and electromagnetic waves in plasmas, in Ref. 61 and 62 respectively, hence lengthy details will be omitted here.

The system's state  $\mathbf{S}$  is expanded as

$$\begin{aligned} \mathbf{S} &= \mathbf{S}^{(0)} + \epsilon \mathbf{S}^{(1)} + \epsilon^2 \mathbf{S}^{(2)} + \dots \\ &= \mathbf{S}^{(0)} + \sum_{n=1}^{\infty} \epsilon^n \mathbf{S}^{(n)} \end{aligned} \quad (9)$$

where  $S^{(0)} = (1, 0, 0; 0, 0; 0, 0)$  demonstrates the equilibrium state of the system and  $\epsilon \ll 1$  is a dimensionless, real and small parameter.

We now introduce new independent spatial and temporal variables,  $x_m = \epsilon^m x$ ,  $t_m = \epsilon^m t$  ( $m = 0, 1, 2, \dots$ ), and accordingly expand the space and time derivative operators  $\partial_x = \partial_{x_0} + \epsilon \partial_{x_1} + \dots$  and  $\partial_t = \partial_{t_0} + \epsilon \partial_{t_1} + \dots$ . Now, we use the assumption that the wavenumber  $k$  and the frequency  $\omega$  (fast variables) affect the perturbed state only via the phase  $kx - \omega t$  of the pulse, which are normalized by  $\omega_{pe}$  and  $k_{pe} = \omega/c$ , respectively. On the other hand, the amplitude of various frequency harmonics is assumed to be a slowly varying function in space and time, and will thus assumed to vary only on the slower scales  $(x_2, x_3, \dots; t_2, t_3, \dots)$ . The solutions to be sought of Eqs. (1-7) are therefore expressed in the form:

$$\mathbf{S}^{(n)} = \sum_{\ell=-\infty}^{\ell=\infty} \mathbf{S}^{(n\ell)}(x_{m \geq 1}, t_{m \geq 1}) e^{i\ell(kx - \omega t)}. \quad (10)$$

The methodology adopted in this work relies on a Newell type multiscale technique, well known from nonlinear optics (where, interestingly space and time are reversed, hence dispersion occurs in the frequency domain, rather than the wavenumber space). The fundamental aim of the method it to allow for a slow variation of the wavepacket's amplitude (envelope) in space and time. An excitation is considered around the equilibrium state (represented by the zeroth order state in a smallness parameter ( $\epsilon^0$ ), while the linear (harmonic) carrier wave regime is obtained in first order ( $\sim \epsilon^1$ ) and the group velocity frame is defined in the second order ( $\sim \epsilon^2$ ), upon imposing certain compatibility conditions (namely, dictating the annihilation of secular terms occurring in that order). In each order in  $\epsilon$ , a secondary expansion is considered in harmonics, from the zeroth to the n-th harmonic. Within this (tedious but straightforward) scheme, the first harmonic (carrier) amplitudes arise as solutions in the first order, while the second harmonic amplitudes will arise via the second-order second-harmonic amplitudes. Zeroth-order amplitudes will originate from the 2nd order 2nd harmonic expressions, in combination with their 3rd order counterparts. Finally, an evolution equation is obtained for the envelope, by eliminating the secular terms occurring in 3rd order (1st harmonics). Linear analysis is therefore embedded in this analysis, thus generalized to account for the generation of higher harmonics.

Substituting Eqs. (9)-(10) into Eqs. (1)-(-7) and collecting the terms arising in each order in  $\epsilon$ , we obtain the amplitude evolution equations at successive orders.

In order  $\mathcal{O}(\epsilon)$  (linear limit), we have the equations

$$\partial_{t_0} n^{(1)} + \partial_{x_0} u^{(1)} = 0, \quad (11)$$

$$\partial_{t_0} u^{(1)} - \partial_{x_0} \phi^{(1)} = 0, \quad (12)$$

$$\partial_{x_0}^2 \phi^{(1)} - n^{(1)} = 0, \quad (13)$$

$$(\partial_{x_0}^2 - \partial_{t_0}^2) A_y^{(1)} - p_y^{(1)} = 0, \quad (14)$$

$$(\partial_{x_0}^2 - \partial_{t_0}^2) A_z^{(1)} - p_z^{(1)} = 0, \quad (15)$$

$$\partial_{x_0} (p_y^{(1)} - A_y^{(1)}) + \Omega p_z^{(1)} = 0, \quad (16)$$

$$\partial_{x_0} (p_z^{(1)} - A_z^{(1)}) - \Omega p_y^{(1)} = 0. \quad (17)$$

- for the zeroth harmonic ( $\ell = 0$ )

$$n^{(10)} = u^{(10)} = 0, \quad (18)$$

$$p_y^{(10)} = p_z^{(10)} = 0, \quad (19)$$

$$A_y^{(10)} = A_z^{(10)} = 0. \quad (20)$$

- for the first harmonic ( $\ell = 1$ )

$$n^{(11)} = u^{(11)} = 0, \quad (21)$$

$$(\omega^2 - k^2) A_y^{(11)} = p_y^{(11)}, \quad (22)$$

$$(\omega^2 - k^2) A_z^{(11)} = p_z^{(11)}, \quad (23)$$

$$-i\omega (p_y^{(11)} - A_y^{(11)}) = -\Omega p_z^{(11)}, \quad (24)$$

$$-i\omega (p_z^{(11)} - A_z^{(11)}) = \Omega p_y^{(11)}. \quad (25)$$

Considering the first harmonic amplitudes ( $\ell = 1$ ), Eqs. (22)-(25) require an explicit compatibility condition to be adopted, in the form

$$\omega^2 - k^2 = \frac{\omega}{\omega - \alpha\Omega}. \quad (26)$$

One recognizes the dispersion relation for circularly-polarized waves [65]. The solution thus obtained for the first-harmonic amplitudes reads:

$$p_z^{(11)} = i\alpha p^{(11)}, \quad p^{(11)} \equiv p_y^{(11)}. \quad (27)$$

$$A_z^{(11)} = i\alpha A^{(11)}, \quad A^{(11)} \equiv A_y^{(11)}. \quad (28)$$

In order  $\mathcal{O}(\epsilon^2)$ , we have the equations

$$\begin{aligned} & \partial_{t_0} n^{(2)} + \partial_{x_0} u^{(2)} \\ &= -\partial_{t_1} n^{(1)} - \partial_{x_0} (n^{(1)} u^{(1)}) - \partial_{x_1} u^{(1)}, \end{aligned} \quad (29)$$

$$\begin{aligned} & \partial_{t_0} u^{(2)} - \partial_{x_0} \phi^{(2)} \\ &= -\partial_{t_1} u^{(1)} + \partial_{x_1} (\phi^{(1)} + p_y^{(1)} \partial_{x_0} (p_y^{(1)} - A_y^{(1)})) \\ &+ p_z^{(1)} \partial_{x_0} (p_z^{(1)} - A_z^{(1)}), \end{aligned} \quad (30)$$

$$\partial_{x_0}^2 \phi^{(2)} - n^{(2)} = -2\partial_{x_0} \partial_{x_1} \phi^{(1)}, \quad (31)$$

$$\begin{aligned} & (\partial_{x_0}^2 - \partial_{t_0}^2) A_y^{(2)} - p_y^{(2)} \\ &= -2(\partial_{x_0} \partial_{x_1} - \partial_{t_0} \partial_{t_1}) A_y^{(1)} + n^{(1)} p_y^{(1)}, \end{aligned} \quad (32)$$

$$\begin{aligned} & (\partial_{x_0}^2 - \partial_{t_0}^2) A_z^{(2)} - p_z^{(2)} \\ &= -2(\partial_{x_0} \partial_{x_1} - \partial_{t_0} \partial_{t_1}) A_z^{(1)} + n^{(1)} p_z^{(1)}, \end{aligned} \quad (33)$$

$$\begin{aligned} & \partial_{t_0} (p_y^{(2)} - A_y^{(2)}) + \Omega p_z^{(2)} \\ &= -(\partial_{t_1} + u^{(1)} \partial_{x_0}) (p_y^{(1)} - A_y^{(1)}), \end{aligned} \quad (34)$$

$$\begin{aligned} & \partial_{t_0} (p_z^{(2)} - A_z^{(2)}) - \Omega p_y^{(2)} \\ &= -(\partial_{t_1} + u^{(1)} \partial_{x_0}) (p_z^{(1)} - A_z^{(1)}). \end{aligned} \quad (35)$$

Same as in the Ref. [62], in the first harmonic ( $\ell = 1$ ), the condition for annihilation of secular terms leads to  $\partial \cdot / \partial t_1 + v_g \partial \cdot / \partial x_1 = 0$  (for  $\cdot = p_{y/z}^{(1)}$  or  $A_{y/z}^{(1)}$ ), implying that the envelope moves at the group velocity  $v_g = \omega'(k)$ , given by:

$$v_g = \frac{2k(\omega - \alpha\Omega)^2}{2\omega(\omega - \alpha\Omega)^2 + \alpha\Omega}, \quad (36)$$

Following the same procedure in order  $\mathcal{O}(\epsilon^3)$ , and using the variables  $X = x_1 - v_g t_1 \equiv \epsilon(x - v_g t)$  and  $T = t_2 \equiv \epsilon^2 t$ , we derive from the non-secularity condition at  $\mathcal{O}(\epsilon^3)$  the NLS Eq. (37)

$$i \frac{\partial \psi}{\partial \tau} + P \frac{\partial^2 \psi}{\partial \xi^2} + Q |\psi|^2 = 0, \quad (37)$$

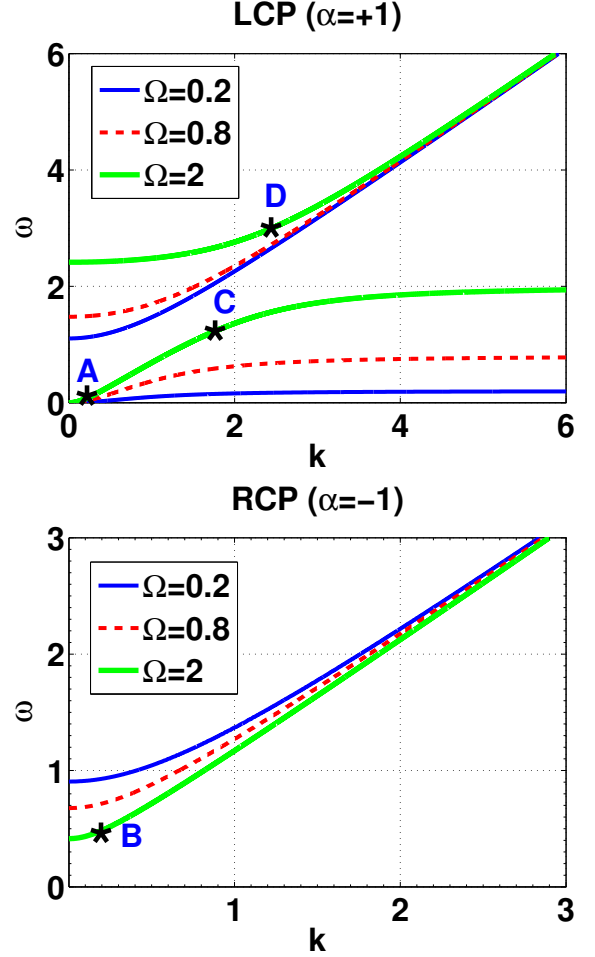


FIG. 1. The dispersion relation showing the frequency  $\omega$  as a function of the wave number  $k$  (normalized values). The different values of  $\Omega$ , i.e.,  $\Omega = 2$ ,  $\Omega = 0.8$ , and  $\Omega = 0.2$  are depicted by bold (green), dashed (red) and thin solid (blue) lines, respectively. Top panel: The LCP EM waves. Bottom panel: The RCP EM waves.

where  $\psi$  denotes the amplitude  $A_y^{(11)}$ , the (slow) time and space variables are  $\tau = t_2$  and  $\xi = x_1 - v_g t_1$ , and the dispersion coefficient  $P$  and the nonlinear self-phase modulation (SPM) coefficient  $Q$  are respectively given by the (real) expressions:

$$P \equiv \frac{1}{2} \frac{\partial^2 \omega}{\partial k^2} = \frac{v_g}{2k} + \frac{v_g^2}{\omega - \alpha\Omega} + \frac{v_g^3 (3\omega - \alpha\Omega)}{2k(\omega - \alpha\Omega)} \quad (38)$$

$$Q = \frac{v_g}{k} (\omega^2 - k^2)^4. \quad (39)$$

#### IV. MULTIPLE SCALE ANALYSIS FOR COUPLED MODES

Now, we consider for a solution in the form

$$S^{(11)} = \sum_{j=1}^2 S_j^{(11)}(x_1, x_2, \dots, t_1, t_2, \dots) \exp(i\theta_j) + \text{c.c.}, \quad (40)$$

where subscripts  $j = 1$  and  $j = 2$  correspond to the LCP and RCP waves,  $S_j^{(11)}$  is an unknown complex function,  $\theta_j = k_j x_0 - \omega_j t_0$ , while the wavenumbers  $k_j$  and frequencies  $\omega_j$  satisfy the dispersion relation provided in Eq. (26). In Fig. 1, we show the dispersion relation for the  $\Omega = 0.2$ ,  $\Omega = 0.8$ , and  $\Omega = 2$ . It is clear, from Fig. 1, that for LCP EM wave (top panel) there exist two frequency bands where the propagation is possible: the high-frequency band and the low-frequency band. For  $\Omega = 0.2$  (depicted by solid (blue) line) the propagation is possible for  $\omega > 1.105$  (high-frequency band) and for  $\omega < 0.2$  (low-frequency band) namely a gap appears between  $0.2 < \omega < 1.105$  where EM wave propagation is not possible. For  $\Omega = 0.8$  (depicted by dashed (red) line) the propagation is possible for  $\omega > 1.477$  (high-frequency band) and for  $\omega < 0.8$  (low-frequency band) where the gap appears between  $0.8 < \omega < 1.477$ . Also, for  $\Omega = 2$  (depicted by thick (green) line) the propagation is possible for  $\omega > 2.414$  (high-frequency band) and for  $\omega < 2$  (low-frequency band). In this case the gap appears between  $2 < \omega < 2.414$ . Moreover, for the RCP EM wave (bottom panel) propagation is possible for frequencies  $\omega > 0.9047$  when  $\Omega = 0.2$  (depicted by solid (blue) line). In case where  $\Omega = 0.8$  (depicted by dashed (red) line) and  $\Omega = 2$  (depicted by thick (green) line) the propagation is possible for frequencies  $\omega > 0.6767$  and  $\omega > 0.414$ , respectively.

Furthermore, the gap which appears for LCP EM waves increases (decreases) as the  $\Omega$  decreases (increases). It is important to notice that there is a frequency region, which is independent from polarization of EM waves, where the propagation cannot take place for values of  $\Omega < 0.707$ .

Below we will demonstrate that in the nonlinear setting, coupling between LCP and RCP EM waves with equal group velocities is possible, and we consider the interaction between LCP and RCP waves. Observing Fig. 1 and knowing that the group velocity at a given wavenumber represents a tangent (line) to the dispersion curve, it is possible to identify domains, with equal group velocities. Thus, using Eq. (26) we obtain the group velocity  $v_g = \partial\omega/\partial k$ :

$$v_g = \frac{2k(\omega - \alpha\Omega)^2}{2\omega(\omega - \alpha\Omega)^2 + \alpha\Omega},$$

i.e. Eq. (36) above.

This result is presented in Fig. 2, where the group velocity  $v_g$  is plotted as a function of the normalized frequency  $\omega$ . Notice that the dashed (red) solid (blue) and

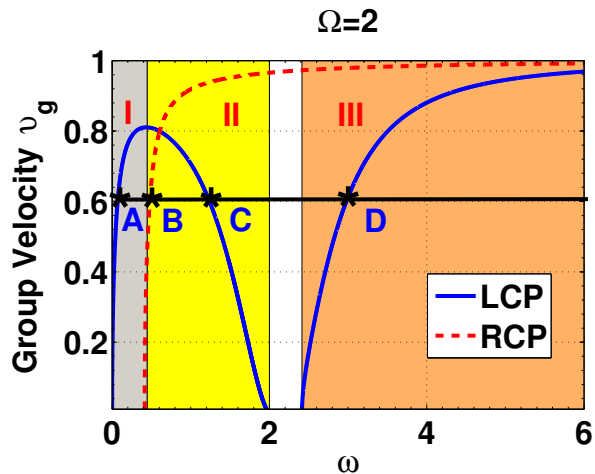


FIG. 2. The group velocity  $v_g$  as a function of the normalized frequency  $\omega$ . The dashed (red) and solid (blue) dashed (red) lines show the group velocity  $v_g$  for RCP- and LCP- EM waves, respectively.

solid (blue) lines show the group velocity  $v_g$  for RCP- and LCP- EM waves, respectively.

As seen in Fig. 2 using a horizontal cut we can observe that there are a RCP and a LCP electromagnetic wave which have the same group velocity (and are coupled in the nonlinear regime).

The point A, B, C and D, in Fig. 2, have the same group velocity, namely,  $v_g = 0.4$ . Also, we see that there is a maximum possible common  $v_{g_{max}}^\ell$  in the low frequency band for LCP wave. Thus, one can divide each of the group-velocity curves into three sub-regions, depending on the sign of the group-velocity dispersion (GVD),  $\partial v_g / \partial \omega$ , where the interaction with equal group velocities may appear. As depicted in Fig. 2 these subregions are: (a) the sub-bands I and II for the low frequency band of the LCP EM wave, characterized by positive and negative GVD respectively, and the sub-bands III for the high frequency band of the LCP EM wave, characterized by positive GVD, (b) the band of the RCP EM wave, again characterized by positive GVD respectively. Thus, nonlinear LCP and RCP modes of equal  $v_g$  can feature the following three different possible interactions:

- *Case 1:* band of the RCP-mode and the LCP-mode in band I, both featuring positive GVD for  $v_g \leq v_{g_{max}}^\ell$ .
- *Case 2:* band of the RCP-mode and the LCP-mode in band II; here, the RCP (LCP) mode features positive (negative) GVD for  $v_g \leq v_{g_{max}}^\ell$ .
- *Case 3:* band of the RCP-mode and the LCP-mode in band III, both featuring positive GVD for  $0 < v_g \leq 1$ .

As shown in Fig. 3, upon inspection of the group-velocity curves for  $\Omega = 0.8$  (middle panel) we see that

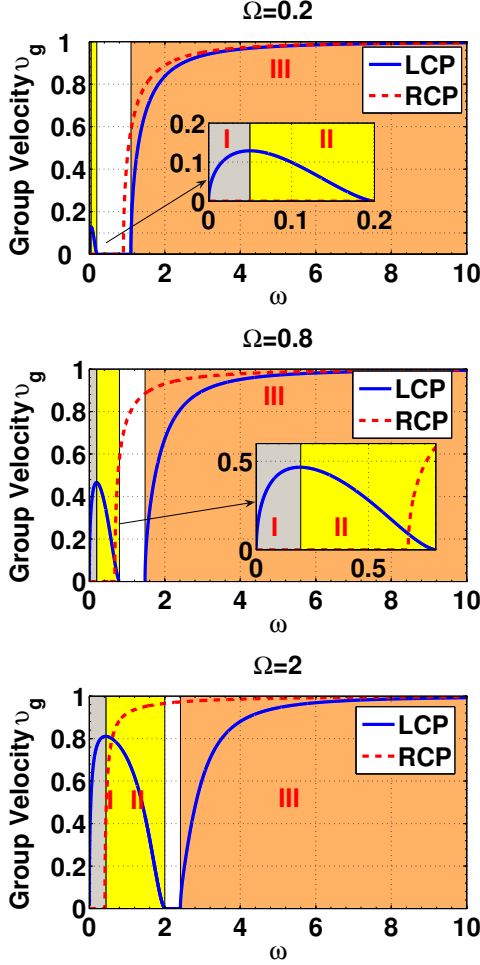


FIG. 3. The group velocity  $v_g$  as a function of the normalized frequency  $\omega$  for different values of  $\Omega$ , i.e.,  $\Omega = 0.2$  (top panel),  $\Omega = 0.8$  (middle panel), and  $\Omega = 2$  (bottom panel). The dashed (red) and solid (blue) dashed (red) lines show the group velocity  $v_g$  for RCP- and LCP- EM waves, respectively.

the maximum possible common  $v_{g_{max}}^\ell = 0.4661$  occurring at  $\omega = 0.198$ , in the low frequency band for LCP wave. Then, the subregions are: (a) the sub-bands I ( $0 < \omega < 0.198$ ) and II ( $0.198 < \omega < 0.8$ ) for the low frequency band and the sub-bands III ( $\omega > 1.477$ ) for the high frequency band of the LCP EM wave (b) the band of the RCP EM wave ( $\omega > 0.6767$ ).

Notice that,  $v_g = 1$  is the group velocity for unmagnetized plasma. It is obvious that the above considerations is the result of the existence of the frequency gap as shows in Fig. 3 for all values of  $\Omega$ , i.e., for  $\Omega = 0.2$ ,  $\Omega = 0.8$  and  $\Omega = 2$ . Furthermore, we can observe that as  $\Omega$  increases the  $v_g^\ell$  is raised and the gap is smaller. When the  $\Omega \gg 1$  then  $v_g \rightarrow 1$  and the LCP and RCP wave are degenerated.

### A. Nonlinear analysis: the coupled NLS equations

In our case, since we study the interaction between a LCP and a RCP nonlinear mode with equal group velocities, we seek for a solution of Eqs. (1-7) in the form:

$$S^{(n)} = \sum_{j=1}^2 S_j^{(n)}(X, T) \exp(i\theta_j) + \text{c.c.}, \quad (41)$$

where ‘‘c.c.’’ denotes complex conjugate. In Eq. (41), subscripts  $j = 1, 2$  correspond to the LCP and RCP mode,  $S_j^{(n)}(X, T)$  are unknown (continuous) slowly-varying envelope functions depending on the slow scales  $X = \epsilon(x - v_g t)$  (where  $v_g$  is the *common* group velocity) and  $T = \epsilon^2 t$ , while  $\exp(i\theta_j)$ , with  $\theta_j = k_j x - \omega_j t$ , are the carriers of frequencies  $\omega_j$  and wavenumbers  $k_j$ . The  $\epsilon$  is a formal small parameter related to the soliton amplitude (see below). According to Eq. (41), the field  $S_j^{(n)}$  is the leading-order form of a more general ansatz employing multiple time and space scales. In this context, use of a formal multi-scale expansion method leads to a hierarchy of equations at various powers of  $\epsilon$ , which are solved up to the third-order. Indeed, at orders  $\mathcal{O}(\epsilon)$  (linear limit) and  $\mathcal{O}(\epsilon^2)$ , we derive the dispersion relation, Eq. (26), and the group velocity, Eq. (36), respectively. At the order,  $\mathcal{O}(\epsilon^3)$  we obtain the nonlinear coupled NLS equations as

$$i\partial_T \Psi_1 + D_1 \partial_X^2 \Psi_1 + (g_{11} |\Psi_1|^2 + g_{12} |\Psi_2|^2) \Psi_1 = 0, \quad (42)$$

$$i\partial_T \Psi_2 + D_2 \partial_X^2 \Psi_2 + (g_{21} |\Psi_1|^2 + g_{22} |\Psi_2|^2) \Psi_2 = 0, \quad (43)$$

where the amplitude  $\Psi_j$ , the normalized GVD coefficients  $D_j$ , the self-phase modulation (SPM) coefficients  $g_{jj}$ , and the cross-phase modulation (CPM) coefficients  $g_{j,3-j}$  (with  $j = 1, 2$ ) are respectively given by:

$$\Psi_j \equiv A_j^{(11)} \quad (44)$$

$$D_j \equiv \frac{1}{2} \frac{\partial^2 \omega_j}{\partial k_j^2} = \frac{v_g}{2k_j} + \frac{v_g^2}{\omega - \alpha\Omega} - \frac{v_g^3(3\omega - \alpha\Omega)}{2k_j(\omega - \alpha\Omega)} \quad (45)$$

$$g_{jj} = \frac{v_g}{k_j} (\omega_j^2 - k_j^2)^4, \quad (46)$$

$$g_{j,3-j} = \frac{2v_g}{k_j} (\omega_j^2 - k_j^2)^2 (\omega_{3-j}^2 - k_{3-j}^2)^2. \quad (47)$$

Note that, using the Eqs. (26) and (36) the above relations be cast in the form:

$$g_{jj} = \frac{2\omega_j^4}{[2\omega_j(\omega_j - \alpha\Omega)^2 + \alpha\Omega](\omega_j - \alpha\Omega)^2}, \quad (48)$$

$$g_{j,3-j} = \frac{4\omega_j^2 \omega_{3-j}^2}{[2\omega_j(\omega_j - \alpha\Omega)^2 + \alpha\Omega](\omega_{3-j} - \alpha\Omega)^2} \quad (49)$$

As shown from Eqs. (46)-(47) the coefficients  $g_{jj}$ , and  $g_{j,3-j}$  are always positive. Next, using scale transformations, we measure normalized time  $T$  and densities  $|\Psi_j|^2$  in units of  $|D_1|^{-1}$  and  $|D_1/g_{jj}|$  respectively, and cast

Eqs. (42)-(43) in the form:

$$i\partial_T\Psi_1 + s\partial_X^2\Psi_1 + (\Psi_1|^2 + \lambda_1|\Psi_2|^2)\Psi_1 = 0, \quad (50)$$

$$i\partial_T\Psi_2 + d\partial_X^2\Psi_2 + (\lambda_2|\Psi_1|^2 + \Psi_2|^2)\Psi_2 = 0, \quad (51)$$

where

$$s = \text{sign}(D_1), \quad d = \frac{D_2}{|D_1|},$$

$$\lambda_1 = \frac{g_{12}}{|g_{22}|}, \quad \lambda_2 = \frac{g_{21}}{|g_{11}|}. \quad (52)$$

where the coefficients  $\lambda_{1,2}$  and  $d$  are positive. As arises from Eqs. (50) when the coupling coefficients ( $\lambda_j = 0$ ) are zero then the evolution of either the LCP wave  $\Psi_1$  or the RCP wave  $\Psi_2$  is described by a single NLS equation; the latter, supports soliton solutions of the dark or the bright type, depending on the relative signs of dispersion and nonlinearity coefficients (see, e.g., Ref. [70]). Particularly, the mode  $\Psi_1$  supports dark solitons for  $s < 0$  or bright solitons for  $s > 0$ . The mode  $\Psi_2$  supports only bright solitons because the coefficient  $d$  is always positive. However, because the above conditions are modified when  $\lambda_j \neq 0$  various types of vector (coupled) solitons can be found as seen from the Eqs. (50) and (51).

According to the Ref. [71], four types of vector solitons are possible:

- *bright-bright* (BB) solitons, in the form:

$$\Psi_1(X, T) = \Psi_{1,0}\text{sech}(bX)\exp(-i\eta_1 T), \quad (53)$$

$$\Psi_2(X, T) = \Psi_{2,0}\text{sech}(bX)\exp(-i\eta_2 T). \quad (54)$$

- *bright-dark* (BD) solitons, in the form:

$$\Psi_1(X, T) = \Psi_{1,0}\text{sech}(bX)\exp(-i\eta_1 T), \quad (55)$$

$$\Psi_2(X, T) = \Psi_{2,0}\tanh(bX)\exp(-i\eta_2 T), \quad (56)$$

- *dark-bright* (DB) solitons, in the form:

$$\Psi_1(X, T) = \Psi_{1,0}\tanh(bX)\exp(-i\eta_1 T), \quad (57)$$

$$\Psi_2(X, T) = \Psi_{2,0}\text{sech}(bX)\exp(-i\eta_2 T), \quad (58)$$

- *dark-dark* (DD) solitons, in the form:

$$\Psi_1(X, T) = \Psi_{1,0}\tanh(bX)\exp(-i\eta_1 T), \quad (59)$$

$$\Psi_2(X, T) = \Psi_{2,0}\tanh(bX)\exp(-i\eta_2 T). \quad (60)$$

In the above equations,  $\eta_j$  ( $j=1,2$ ) and  $\Psi_{j,0}$  declare the frequencies and amplitudes of each soliton, while  $b$  is the (common) inverse width of the solitons.

Now, each of the above ansatz is substituted in Eqs. (50) and (51), leading to a set of equations connecting the soliton parameters. Particularly, the equations connecting the amplitudes  $\Psi_{j,0}$  and the inverse width  $b$  are of the form:

$$(\Psi_{2,0}/\Psi_{1,0})^2 = -\alpha_1, \quad (b/\Psi_{1,0})^2 = -\alpha_2, \quad (61)$$

$$(\Psi_{2,0}/\Psi_{1,0})^2 = \alpha_1, \quad (b/\Psi_{1,0})^2 = -\alpha_2, \quad (62)$$

$$(\Psi_{2,0}/\Psi_{1,0})^2 = \alpha_1, \quad (b/\Psi_{1,0})^2 = \alpha_2, \quad (63)$$

$$(\Psi_{2,0}/\Psi_{1,0})^2 = -\alpha_1, \quad (b/\Psi_{1,0})^2 = \alpha_2, \quad (64)$$

for the BB, BD, DB and DD solitons respectively, where parameters  $\alpha_j$  ( $j = 1, 2$ ) are given by:

$$\alpha_1 = \frac{s\lambda_2 - d}{s - d\lambda_1}, \quad \alpha_2 = \frac{\lambda_1\lambda_2 - 1}{2(s - d\lambda_1)}. \quad (65)$$

It is worth noting that a similar set of coupled NLS equation has been derived in the past for modulational wavepacket interaction in electron-ion plasmas, considering either upper-hybrid [72] or, more recently, electrostatic [73–75] waves. Although the mathematical setting is analogous, and may therefore interest the reader of this paper, the physical background in this paper is distinct from those works; in those earlier studies, for instance, an unmagnetized plasma was considered, in the electrostatic approximation (i.e. neglecting magnetization, thus precluding electromagnetic excitations), with the focus being on the nonthermal (kappa-distributed) background electron statistics (a common occurrence in Space plasmas). Contrary to that picture, our focus here is on electromagnetic solitary waves propagating in magnetized plasma and, in particular, on the role of the ambient magnetic field on their structural and propagation characteristics.

## V. SOLITON INTERACTIONS IN DIFFERENT FREQUENCY BANDS

It is important to understand that the sign of the parameters  $\alpha_j$  ( $j = 1, 2$ ) defined above determines the type of vector solitons that may occur in the plasma, as dictated by Eqs. (61)-(64). Also, the parameters  $\alpha_j$  depend on the frequency and the magnetic field according to Eq. (65), through coefficients  $\lambda_{1,2}$ ,  $s$  and  $d$ . Consequently, we expect that the precise solitons solutions will arise from the investigation of the sign of the parameters  $\alpha_j$  and the value of magnetic field, for all cases (Case 1, 2 and 3) as have been defined in Section V. On the other hand, the Eqs. (50)-(51) are no longer of the Manakov type and, thus, generally, they are not completely integrable. Nevertheless, standing wave soliton solutions whose exact analytical form depend on by sign of the parameters  $\alpha_j$  can still be found. That is valid for all cases of interactions (Case 1, 2, and 3).

### A. Case 1: Solitons in bands I and RCP.

Initially, we study the coupling between a propagating soliton, with a frequency that is in band I, and a propagating soliton, with a frequency that is in RCP band. In Fig. 4 we depict the dependence of the parameters  $\lambda_1$ ,  $\lambda_2$  and  $d$ , as a function of the normalized frequency  $\omega$  (for  $\Omega = 0.2$ ,  $\Omega = 0.8$  and  $\Omega = 2$ ). Now, we have  $s = +1$  (cf. Fig. 3) and  $\lambda_{1,2} > 0$  and  $d > 0$ , as can be seen in the

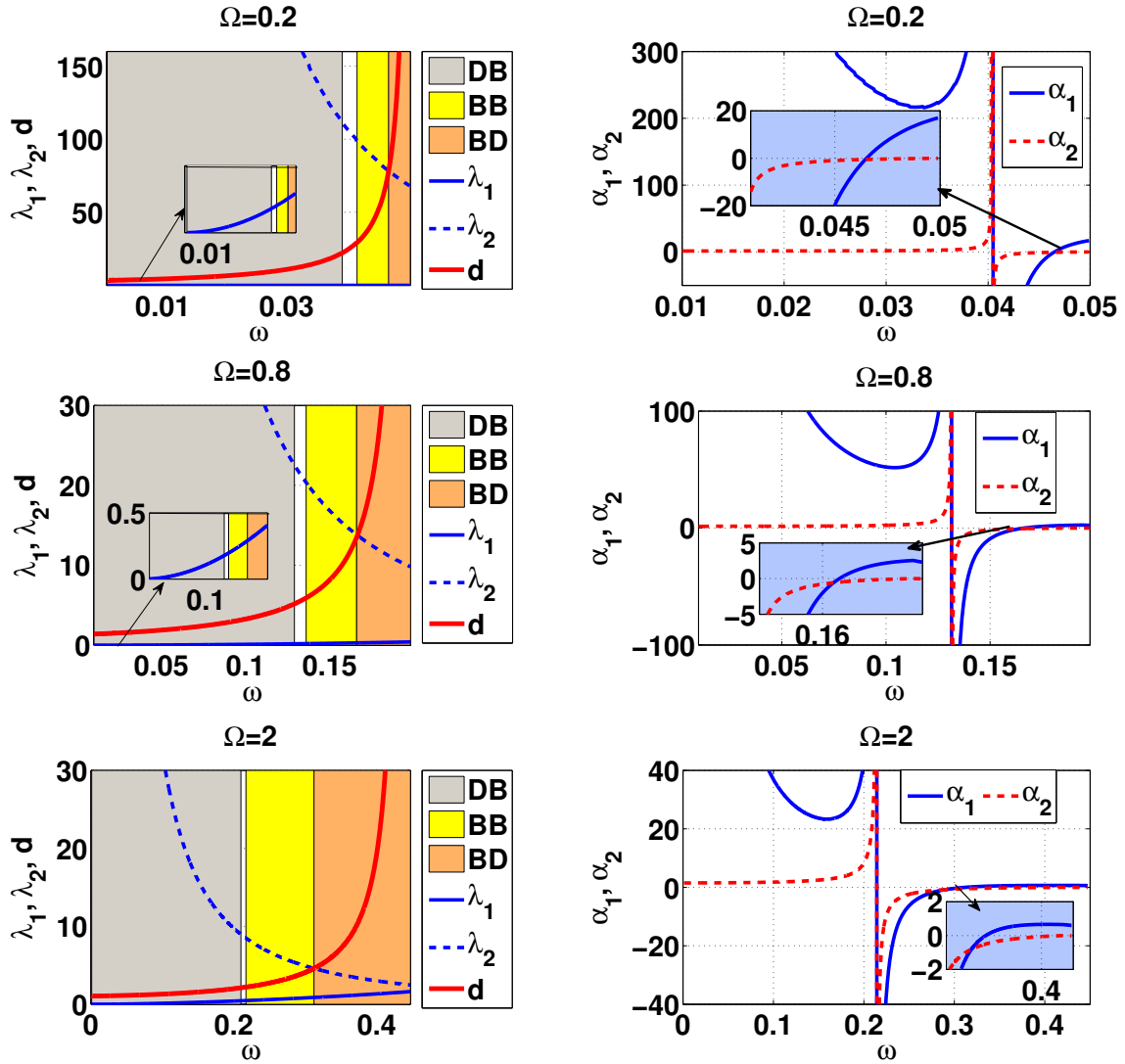


FIG. 4. Case 1: (Left panels) The dependence of the parameters,  $\lambda_1$  [thin solid (blue) line],  $\lambda_2$  [dashed (blue) line] and  $d$  [bold solid (red) line] on the normalized frequency  $\omega$ , for different values of  $\Omega$ , i.e.,  $\Omega = 0.2$  (top panel),  $\Omega = 0.8$  (middle panel), and  $\Omega = 2$  (bottom panel). (Right panels) The same for the coefficients  $\alpha_1$  [solid (blue) line],  $\alpha_2$  [dashed (red) line].

Fig. 4. Also, the parameters  $\alpha_j$  ( $j = 1, 2$ ) are given by:

$$\alpha_1 = \frac{\lambda_2 - d}{1 - d\lambda_1}, \quad (66)$$

$$\alpha_2 = \frac{\lambda_1\lambda_2 - 1}{2(1 - d\lambda_1)}. \quad (67)$$

In this case, the Eqs. (50)-(51) are no longer of the Manakov type and, thus, generally, they are not completely integrable. Nevertheless, standing wave solitons solutions can still be found whose exact analytical form depend on by sign of the parameters  $\alpha_j$ . 1. When  $\alpha_1 > 0$  and  $\alpha_2 > 0$  then we have a case of coupled solitons, a dark soliton and a bright soliton, whose exact analytical form are given by Eqs. (57)-(58), where the soliton amplitude parameters  $\eta_{1,2}$  and the inverse width  $b$  are connected

via the following equations:

$$\eta_1 = -\Psi_{1,0}^2, \quad (68)$$

$$\eta_2 = -(d\alpha_2 + \lambda_2)\Psi_{1,0}^2, \quad (69)$$

$$b^2 = \alpha_2\Psi_{1,0}^2, \quad (70)$$

It is thus clear that the above solutions have one free parameter. Employing the solutions (57)-(58), we can approximate the vector potential  $A_y(x, t)$ , in terms of the original coordinates  $x$  and  $t$ , as follows:

$$A_y(x, t) \approx A_{y0}[\Psi_1(x, t) \cos(k_1x - \omega_01t) + \Psi_2(x, t) \cos(k_2x - \omega_02t)], \quad (71)$$



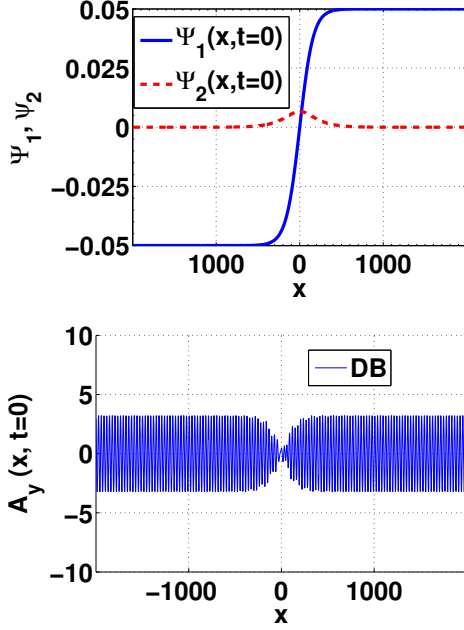


FIG. 5. Case 1: The profiles (at  $t=0$ ) of the dark and bright solitons (top panel) and dark-bright soliton (bottom panel) for  $\Omega = 0.8$ . The parameters used are  $v_g = 0.2965$ ,  $\omega_1 = 0.0335$  ( $k_1 = 0.2119$ ) and  $\omega_2 = 0.7007$  ( $k_2 = 0.1551$ ). Also, we use  $\epsilon = 0.1$  and  $\Psi_{1,0} = 0.05$ .

The amplitude  $A_0$  and the frequencies  $\omega_{0j}$  ( $j = 1, 2$ ) of the soliton are given by:

$$A_{y0} = 2\epsilon \sqrt{\left| \frac{D_1}{g_{11}} \right|}, \quad (72)$$

$$\omega_{0j} = \omega_j + \epsilon^2 \eta_j |D_1|. \quad (73)$$

In this case,

$$\Psi_1 = \Psi_{1,0} \tanh[\epsilon b(x - v_g t)], \quad (74)$$

$$\Psi_2 = \sqrt{\left| \frac{g_{11}}{g_{22}} \right|} \alpha_1 \Psi_{1,0} \operatorname{sech}[\epsilon b(x - v_g t)]. \quad (75)$$

In Fig. 5 we show the profiles (at  $t=0$ ) of the dark (LCP mode) and bright (RCP mode) solitons in the absence of coupling (top panel) as well as the dark-bright soliton (bottom panel), for  $\Omega = 0.8$ . Now, the group velocity of the DB soliton (common for both components) is  $v_g = 0.2965$ , which occurs when the angular frequencies for the modes  $\Psi_1$  and  $\Psi_2$  take, respectively, the values  $\omega_1 = 0.0335$  ( $k_1 = 0.2119$ ) and  $\omega_2 = 0.7007$  ( $k_2 = 0.1551$ ).

**2.** When  $\alpha_1 < 0$  and  $\alpha_2 < 0$  then we have a case of coupled bright solitons, whose exact analytical form are given by Eqs. (53)-(54). Now, the parameters  $\eta_{1,2}$  and  $b$  are connected via the following equations:

$$\eta_1 = \alpha_2 \Psi_{1,0}^2, \quad (76)$$

$$\eta_2 = d\alpha_2 \Psi_{1,0}^2, \quad (77)$$

$$b^2 = -\alpha_2 \Psi_{1,0}^2. \quad (78)$$

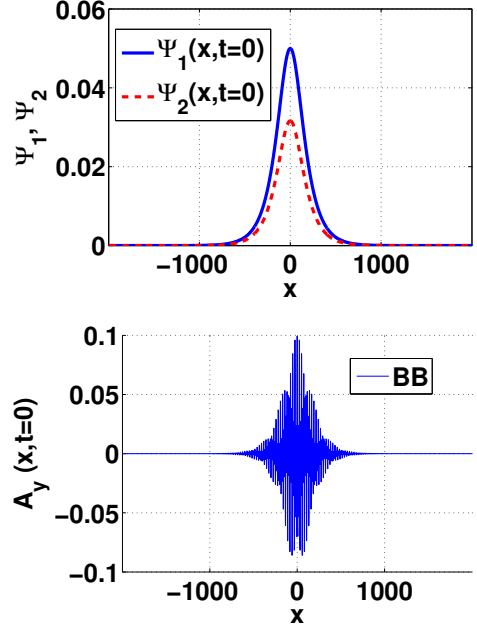


FIG. 6. Case 1: The profiles (at  $t=0$ ) of the bright solitons (top panel) and dark-bright soliton (bottom panel) for  $\Omega = 0.8$ . The parameters used are  $v_g = 0.4572$ ,  $\omega_1 = 0.1454$  ( $k_1 = 0.4932$ ) and  $\omega_2 = 0.77414$  ( $k_2 = 0.2621$ ). Also, we use  $\epsilon = 0.1$  and  $\Psi_{1,0} = 0.05$ .

The vector potential  $A_y(x, t)$ , in terms of the original coordinates  $x$  and  $t$  and soliton parameters, are given by the Eq. (71) and Eqs. (72)-(73) respectively, where, now

$$\Psi_1 = \Psi_{1,0} \operatorname{sech}[\epsilon b(x - v_g t)], \quad (79)$$

$$\Psi_2 = \sqrt{\left| \frac{g_{11}}{g_{22}} \right|} \alpha_1 \Psi_{1,0} \operatorname{sech}[\epsilon b(x - v_g t)]. \quad (80)$$

In Fig. 6 we show the profiles (at  $t=0$ ) of the bright (LCP mode) and bright (RCP mode) solitons in the absence of coupling (top panel) as well as the bright-bright soliton (bottom panel), for  $\Omega = 0.8$ . Now, the group velocity of the BB soliton (common for both components) is  $v_g = 0.4572$ , which occurs when the angular frequencies for the modes  $\Psi_1$  and  $\Psi_2$  take, respectively, the values  $\omega_1 = 0.1454$  ( $k_1 = 0.4932$ ) and  $\omega_2 = 0.77414$  ( $k_2 = 0.2621$ ).

**3.** When  $\alpha_1 > 0$  and  $\alpha_2 < 0$  then we have a case of coupled solitons, a bright soliton and a dark soliton, whose exact analytical form are given by Eqs. (55)-(56), where the soliton amplitude parameters  $\eta_{1,2}$  and the inverse width  $b$  are connected via the following equations:

$$\eta_1 = (\alpha_2 - \alpha_1 \lambda_1) \Psi_{1,0}^2, \quad (81)$$

$$\eta_2 = -\alpha_1 \Psi_{1,0}^2, \quad (82)$$

$$b^2 = -\alpha_2 \Psi_{1,0}^2. \quad (83)$$

Now, we can approximate the vector potential  $A_y(x, t)$ , in terms of the original coordinates  $x$  and  $t$ , as in the

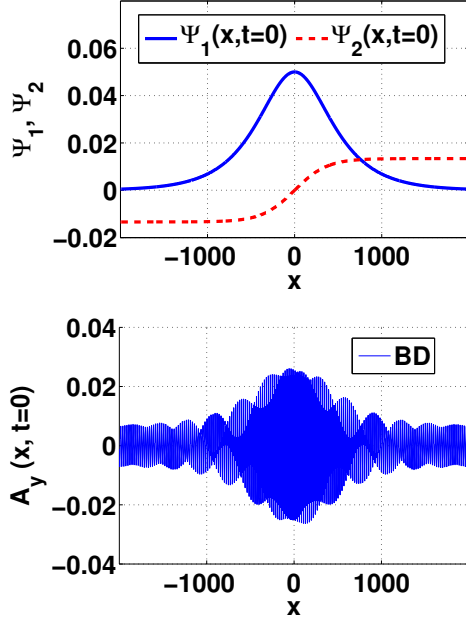


FIG. 7. Case 1: The profiles (at  $t=0$ ) of the bright and dark solitons (top panel) and bright-dark soliton (bottom panel) for  $\Omega = 0.8$ . The parameters used are  $v_g = 0.4647$ ,  $\omega_1 = 0.1743$  ( $k_1 = 0.5558$ ) and  $\omega_2 = 0.744$  ( $k_2 = 0.2677$ ). Also, we use  $\epsilon = 0.1$  and  $\Psi_{1,0} = 0.05$ .

Eq. (71) where, in this case,

$$\Psi_1 = \Psi_{1,0} \operatorname{sech}[\epsilon b(x - v_g t)], \quad (84)$$

$$\Psi_2 = \sqrt{\left| \frac{g_{11}}{g_{22}} \right|} \alpha_1 \Psi_{1,0} \tanh[\epsilon b(x - v_g t)]. \quad (85)$$

In this case, the solution amplitude  $A_0$  and the frequencies  $\omega_{0j}$  ( $j = 1, 2$ ) are given by Eqs. (72)-(73).

In Fig. 7 we show the profiles (at  $t=0$ ) of the bright (LCP mode) and dark (RCP mode) solitons in the absence of coupling (top panel) as well as the bright-dark soliton (bottom panel), for  $\Omega = 0.8$ . Now, the group velocity of the BD soliton (common for both components) is  $v_g = 0.4647$ , which occurs when the angular frequencies for the modes  $\Psi_1$  and  $\Psi_2$  take, respectively, the values  $\omega_1 = 0.1743$  ( $k_1 = 0.5558$ ) and  $\omega_2 = 0.744$  ( $k_2 = 0.2677$ ).

**TABLE 1**

		$\alpha_1$	
		-	+
$\alpha_2$	-	BB	BD
	+		DB

The above table shows the existence of vector solitons according to the sign of the coefficients  $\alpha_1$  and  $\alpha_2$ , for the case 1. Moreover, as are depicted in Fig. 4, for  $\Omega = 0.8$ , the above solutions are defined only for a narrow frequency band (0–0.129), (0.136–0.166) and (0.17–0.198) for dark-bright (DB), bright-bright (BB) and bright-dark (BD) interactions, respectively. Also, as is observed in

the Fig. 4, as  $\Omega$  is decreased (increased) lead to an increase (decrease) of the width of the DB band where DB solitons can be formed, while the width of BB and BD band is decreased (increased). As seen in this figure, for  $\Omega = 0.2$  the DB, BB and BD band possess, approximately, the 80%, 10% and 6% of I-band, respectively. Notice that for  $\Omega = 0.8$  ( $\Omega = 2$ ) the DB, BB and BD band possess, the 65% (47%), 15% (21%) and 14% (30%) of I-band, respectively.

### B. Case 2: Bright-dark solitons in bands II and RCP.

In this case  $s = -1$ , we study the coupling between a propagating soliton, with a frequency that is in band II, and a propagating soliton, with a frequency that is in RCP band. In Fig. 8 we depict the dependence of the parameters  $\lambda_1$ ,  $\lambda_2$  and  $d$ , as a function of the normalized frequency  $\omega$  (for  $\Omega = 0.2$ ,  $\Omega = 0.8$  and  $\Omega = 2$ ). Now, the coefficients  $\alpha_1$  and  $\alpha_2$  take the following form:

$$\alpha_1 = \frac{\lambda_2 + d}{1 + d\lambda_1}, \quad (86)$$

$$\alpha_2 = -\frac{\lambda_1 \lambda_2 - 1}{2(1 + d\lambda_1)}. \quad (87)$$

Following our previous considerations, here we have a case of coupled bright-dark solitons where the exact analytical form is given by Eqs. (55)-(56). The soliton amplitude parameters  $\eta_{1,2}$  and the inverse width  $b$  are connected via the following equations:

$$\eta_1 = -(\alpha_2 + \alpha_1 \lambda_1) \Psi_{1,0}^2, \quad (88)$$

$$\eta_2 = -\alpha_1 \Psi_{1,0}^2, \quad (89)$$

$$b^2 = -\alpha_2 \Psi_{1,0}^2. \quad (90)$$

The analytical form for vector potential  $A_y(x, t)$  and the solitons parameters are same with the previous case, namely, in the interaction in bands I and RCP [c.f. Eqs. (84)-(85)].

### C. Case 3: Solitons in bands III and RCP.

Finally, we study the coupling between a propagating soliton, with a frequency that is in band III, and a propagating soliton, with a frequency that is in RCP band. Now,  $s = +1$  (cf. Fig. 3) while the other dispersion and nonlinearity coefficients are shown in Fig. 9 as functions of the normalized frequency  $\omega$  for  $\Omega = 0.2$ ,  $\Omega = 0.8$  and  $\Omega = 2$ . Also, as is observed in the Fig. 9, as  $\Omega$  is increased lead to an increase of the width of the BD band where BD solitons can be formed, while the width of BB is decreased.

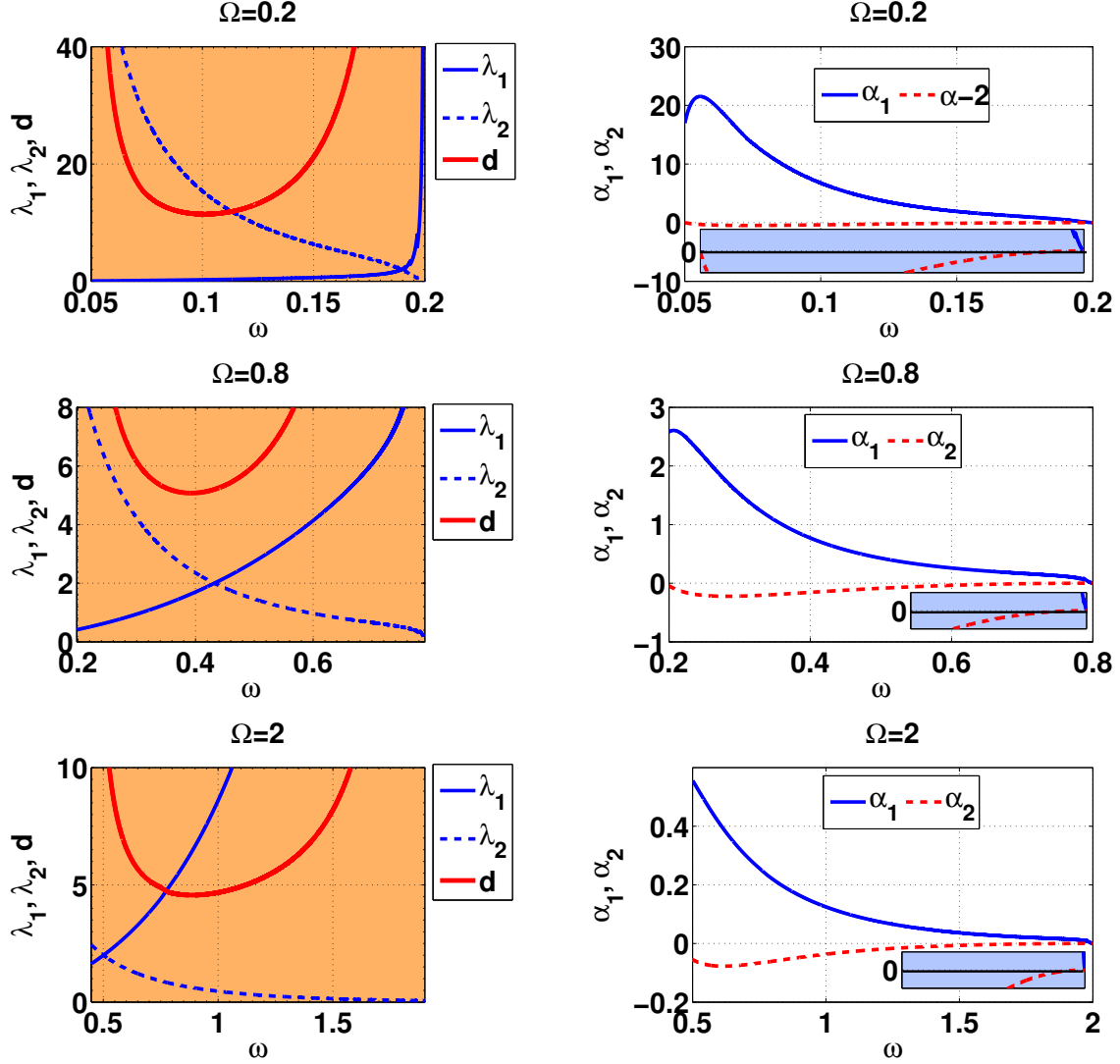


FIG. 8. Same as Fig. 4, but for Case 2.

#### D. Discussions

The analysis of previous section end in some important results which confirm our expectations. First of all in the Case 1 (Solitons in bands I and RCP) we obtain three types of vector solitons, namely bright-bright, bright-dark and dark-bright. Also, we observe that for low frequencies and  $\Omega$  values the width of the dark-bright band where dark-bright solitons can be formed possesses the larger percentage of the band. However as  $\Omega$  is increased the occurrence of the dark-bright type is decreased while the width of the bright-bright and mainly also that of the bright-dark category are increased. In Case 2 (Case 2: Bright-dark solitons in bands II and RCP) for all the frequencies and  $\Omega$  values, we have only the existence of bright-dark solitons. Finally, in Case 3 (Solitons in bands III and RCP) we have only bright-bright solitons in all the frequencies for low  $\Omega$  values. As  $\Omega$  is increased bright-

dark solitons appeared which dominate in all frequency band for the large values of  $\Omega$ .

According to the table in Fig. 10, we found that bright-dark solitons exist in all frequency bands for all values of  $\Omega$ . Furthermore, we observe bright-bright solitons in bands (I-RCP) and (III-RCP) for the small values of  $\Omega$ . Also, we found that the dark-bright solitons exist only in I-RCP frequency band for small values of  $\omega$  and  $\Omega$ .

Generally our detailed analysis can support various coupled NLS systems in magnetized plasmas with the equal group velocities between the propagating waves. Our analytical investigation reveals the existence of various type vector solitons taking into account the certain frequency bands and the strength of the magnetic field. It is very important to note that from our suggested method the capability control of a solitonic mode e.g. LCP (RCP) from the change the amplitude or width of other mode RCP (LCP) emerges.

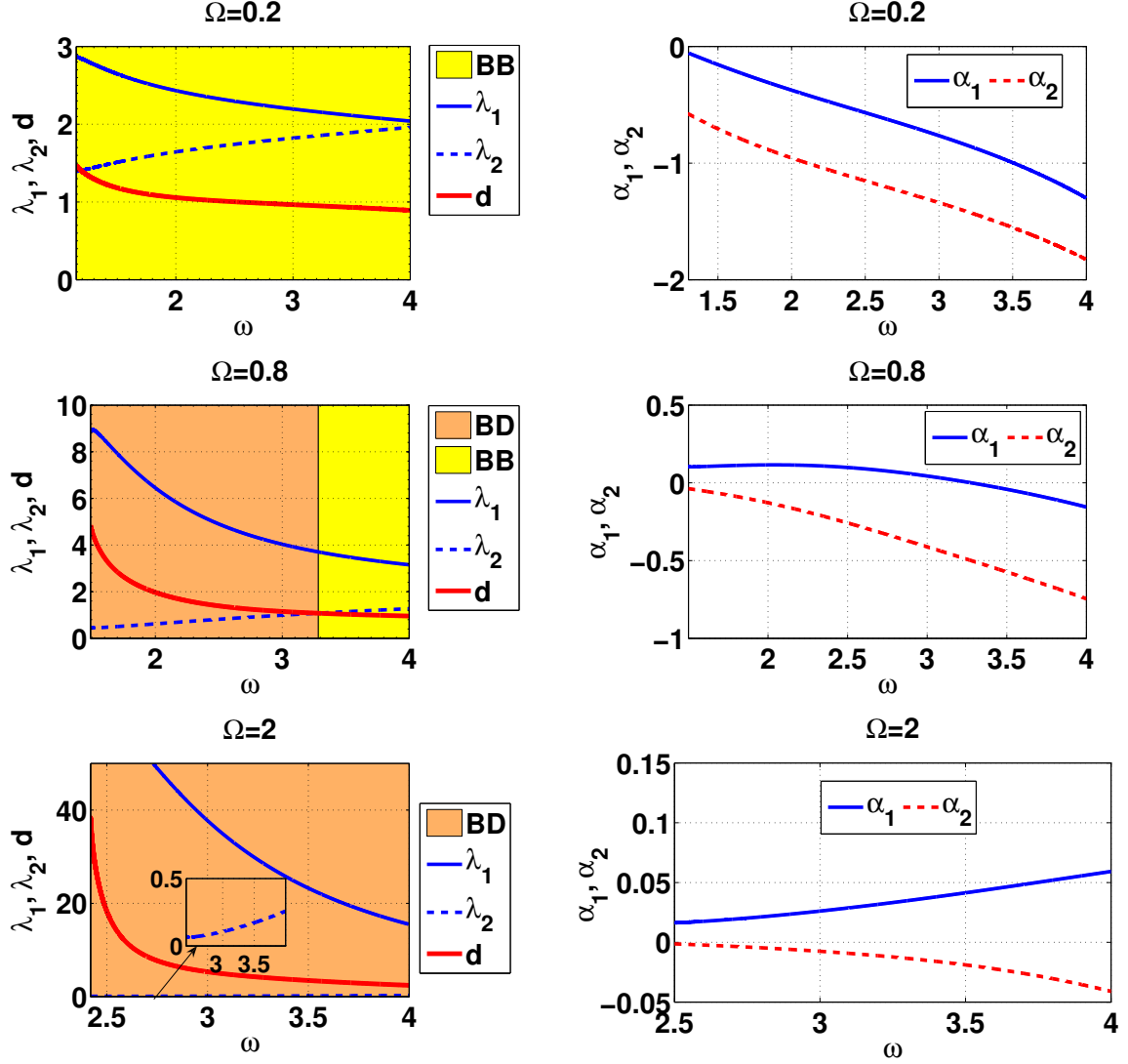


FIG. 9. Same as Fig. 4, but for Case 3.

Although our present work has an analogous mathematical settings with the works of Refs. [62], [71], [73], and [75] it has serious differences as: a) The physical background in this paper is different compared to Refs. [71], [73], and [75]. In Refs. [73] and [75] the study was carried out in the framework of an unmagnetized plasma while in the Ref. [71] the physical background was completely different where a nonlinear composite right left handed transmission line was studied, b) With regards to Ref. [62], where the physical background is same, namely the magnetized plasma, in this paper we study the interaction between left hand circularly polarized (LCP) and right hand circularly polarized (RCP) solitons while in Ref. [62], we investigated only the beam-plasma interaction, c) As previously mentioned, in this paper, we investigate the interaction between of a LCP and RCP electromagnetic wave which have the same group velocity in different frequency bands. In Refs [73] and [75]

the electrostatic wave packets are studied in a regime with different group velocities, d) In this work, we study the vector soliton solutions in different frequency bands and for different magnetic fields. The analysis in Ref. [71] was carried out only for different frequency bands, in Ref. [73], the instability growth rate was investigated while in the Ref. [75], the analysis was focused on the values of the  $\kappa$ -index of k-distribution function.

## VI. CONCLUSION

In conclusion, we have performed analytical techniques to study the existence of coupled left- and right-circularly polarized solitons in magnetized plasmas. Our analysis started with the derivation of a closed system of scalar equations which govern the propagation of LCP and RCP EM waves in magnetized plasmas. Upon the

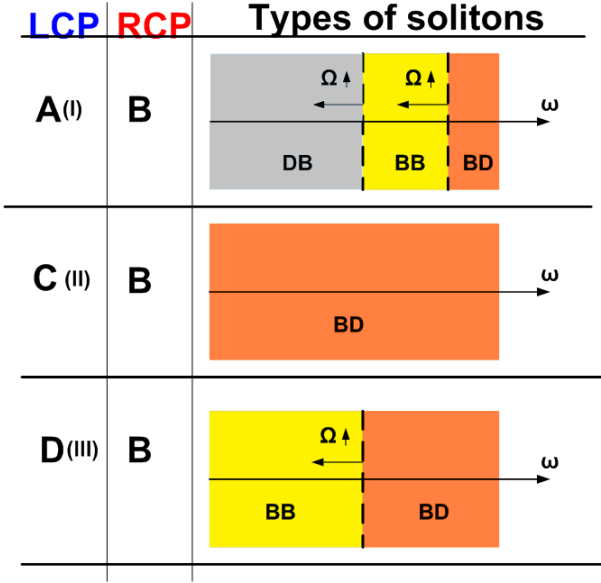


FIG. 10. Different types of solitons as a function of the angular (normalized) frequency  $\omega$  are depicted in the table, for the different values of  $\Omega$ .

linear limit, the dispersion relation has been derived and we have shown that there are LCP- and RCP modes, with the same group velocity, which can be propagate for specific frequency bands. Next, in the nonlinear regime we used the multiple scale perturbation method in order to investigated the coupling between LCP- and RCP modes. In this framework, we obtain, a system of two coupled nonlinear Schrödinger (NLS) equations for the unknown vector potential envelope functions. The above system of equations was used in order to predict the existence of coupled left- and right-circularly polarized solitons in magnetized plasmas, of the bright-bright, bright-dark and dark-bright type.

Thus, we found vector solitons of the same type (namely, bright-bright) as well as ones of the mixed type (namely, bright-dark and dark-bright) in specific frequency bands. Also, the values of  $\Omega$  change the width of frequency band where the vector solitons can be formed. Thus, we found vector solitons of the type dark-bright, bright-bright and bright-dark in the bands I and RCP where the increase of the  $\Omega$  lead to a decrease of the width of the band of dark-bright solitons with simulta-

neous increase of the width of the band of the bright-bright and bright-dark solitons. In the bands II and RCP only bright-dark solitons were found. Finally, we found bright-dark and bright-bright solitons in the bands III and RCP where the increase of the  $\Omega$  lead to a decrease of the width of the band of bright-bright solitons with simultaneous increase of the width of the band of the bright-dark solitons.

Our results should be of interest to the plasma science community, where beam-plasma interactions are a hot topic of research nowadays, both theoretically and in the laboratory (laser plasma interaction experiments), and also in nonlinear optics, where coupled beam propagation is an ubiquitous point of focus. Beyond these physical settings, coupled NLS equations such as our Eqs. (24)-(25) arise in various contexts, ranging from hydrodynamics to superconductivity (Bose-Einstein condensates) and left-hand materials, to mention a few. The mathematical setting and the methodology of our study is thus expected to apply in a wider context.

#### ACKNOWLEDGEMENTS

Author IK and NL gratefully acknowledges financial support from Khalifa University (United Arab Emirates) via the project CIRA-2021-064 (8474000412). IK also acknowledges support from KU via the project FSU-2021-012 (8474000352), as well as from KU Space and Planetary Science Center (KU SPSC), Abu Dhabi, United Arab Emirates, via grant No. KU-SPSC-8474000336.

This work was completed during a research visit by author IK to the Physics Department, National and Kapodistrian University of Athens, Greece. During the same period, author IK also held an Adjunct Researcher status at the Hellenic Space Center, Greece. The hospitality of both hosts, represented by Professor D.J. Frantzeskakis and (HSC Director) Professor I. Daglis, respectively, is warmly acknowledged.

Author GV acknowledges support from ADEK (Abu Dhabi Education and Knowledge Council, currently ASPIRE-UAE) AARE (Abu Dhabi Award of Research Excellence) grant (AARE18-179) during a research visit in 2022. Hospitality from the host (Khalifa University) during that visit is gratefully acknowledged.

- [1] Akhiezer, A., Polovin, R.V.: Theory of wave motion of an electron plasma. *Zh. Eksp. Teor. Fiz.* **30**, 915 (1956) [*Sov. Phys. JETP* **3**, 696 (1956)]
- [2] Kozlov, V.A., Litvak, A.G., Suvorov, E.V.: Envelope solitons of relativistic strong electromagnetic waves. *Soviet Phys. JETP* **49**, 75–80 (1979)
- [3] Kaw, P.K., Sen, A., Katsouleas, T.: Nonlinear 1D laser pulse solitons in a plasma. *Phys. Rev. Lett.* **68**, 3172

- (1992); <https://doi.org/10.1103/PhysRevLett.68.3172>
- [4] Esirkepov, T.Zh., Kamenets, F.F., Bulanov, S.V., Naumova, N.M.: Low-frequency relativistic electromagnetic solitons in collisionless plasmas. *JETP Lett.* **68**, 36 (1998); <https://doi.org/10.1134/1.567817>
- [5] Kruer, W.: *The Physics Of Laser Plasma Interactions* (1st Edition). CRC Press (2003); <https://doi.org/10.1201/9781003003243>.

- [6] Eliezer, S., Mima, K.: Applications of Laser-Plasma Interactions, Series in Plasma Physics (Taylor & Francis, 2009).
- [7] Quesnel, B., Mora, P., Adam, J.C., Héron, A., Laval, G.: Electron parametric instabilities of ultraintense laser pulses propagating in plasmas of arbitrary density. *Phys. Plasmas* **4**, 3358 (1997); <https://doi.org/10.1063/1.872494> ; Barr, H.C., Mason, P., Parr, D.M.: Electron parametric instabilities driven by relativistically intense laser light in plasma. *Phys. Rev. Lett.* **83**, 1606 (1999); <https://doi.org/10.1103/PhysRevLett.83.1606>
- [8] Gleixner, F., and Kumar, N.: Electronic parametric instabilities of an ultrarelativistic laser pulse in a plasma. *Phys. Rev. E* **101**, 033201 (2020); doi:10.1103/physreve.101.033201
- [9] Mori, W.B., Decker, C.D., Leemans, W.P.: Relativistic harmonic content of nonlinear electromagnetic waves in underdense plasmas. *IEEE Trans. Plasma Sci.* **21** (1), 110–119 (1993); DOI: 10.1109/27.221109 Esarey, E., Ting, A., Sprangle, P., Umstadter, D., Liu, X.: Nonlinear analysis of relativistic harmonic generation by intense lasers in plasmas. *IEEE Trans. Plasma Sci.* **21** (1), 95–104 (1993); DOI: 10.1109/27.221107
- [10] Esarey, E., Sprangle, P., Krall, J., Ting, A.: Self-focusing and guiding of short laser pulses in ionizing gases and plasmas. *IEEE J. Quantum Electron.* **33** (11), 1879–1914 (1997); DOI: 10.1109/3.641305
- [11] Borghesi, M., Campbell, D.H., Schiavi, A., Haines, M.G., Willi, O., MacKinnon, A.J., Patel, P., Gizzi, L.A., Galimberti, M., Clarke, R.J., Pegoraro, F., Ruhl, H., Bulanov, S.: Electric field detection in laser-plasma interaction experiments via the proton imaging technique. *Phys. Plasmas* **9**, 2214–2220 (2002); <https://doi.org/10.1063/1.1459457>
- [12] Wagner, U., Tatarakis, M., Gopal, A., Beg, F.N., Clark, E.L., Dangor, A.E., Evans, R.G., Haines, M.G., Mangles, S.P.D., Norreys, P.A., Wei, M.-S., Zepf, M., Krushelnick, K.: Laboratory measurements of 0.7 GG magnetic fields generated during high-intensity laser interactions with dense plasmas. *Phys. Rev. E* **70**, 026401 (2004); <https://doi.org/10.1103/PhysRevE.70.026401>
- [13] Chen, S.-Y., Krishnan, M., Maksimchuk, A., Umstadter, D.: Excitation and damping of a self-modulated laser wakefield. *Phys. Plasmas* **7**, 403–413 (2000); <https://doi.org/10.1063/1.873809>
- [14] Roy, S., Chatterjee, D., and Misra, A. P.: Generation of wakefields and electromagnetic solitons in relativistic degenerate plasmas. *Phys. Scr.* **95**, 015603. (2019); doi:10.1088/1402-4896/ab447d
- [15] Melrose, D.B., McPhedran, R.C.: *Electromagnetic Processes in Dispersive Media*. Cambridge University Press (1991); <https://doi.org/10.1017/CBO9780511600036> .
- [16] Di Piazza, A., Müller, C., Hatsagortsyan, K.Z., Keitel, C.H.: Extremely high-intensity laser interactions with fundamental quantum systems. *Rev. Mod. Phys.* **84**, 1177 (2012); <https://doi.org/10.1103/RevModPhys.84.1177>
- [17] Brodin, G., Marklund, M., Stenflo, L.: Proposal for detection of QED vacuum nonlinearities in Maxwell's equations by the use of waveguides. *Phys. Rev. Lett.* **87** (17), 171801 (2001); <https://doi.org/10.1103/PhysRevLett.87.171801>
- [18] Nargesi, N., Miraboutalebi, S., Rajaei, L., Samavati, K.: The quantum exchange effects on the electromagnetic solitonic excitations in warm plasma. *Results in Physics* **52** 106877 (2023); <https://doi.org/10.1016/j.rinp.2023.106877>
- [19] Bulanov, S. V., Sasorov, P. V., Pegoraro, F., Kadlecov, H., Bulanov, S. S., Esirkepov, T. Zh., Rosanov, N. N., Korn, G.: Electromagnetic Solitons in Quantum Vacuum. *Phys. Rev. D* **101**, 016016 (2020); <https://doi.org/10.1103/PhysRevD.101.016016>
- [20] Macchi, A., Borghesi, M., Passoni, M.: Ion acceleration by superintense laser-plasma interaction. *Rev. Mod. Phys.* **85**, 751 (2013); <https://doi.org/10.1103/RevModPhys.85.751>
- [21] Borghesi, M., Audebert, P., Bulanov, S.V., Cowan, T., Fuchs, J., Gauthier, J.C., Mackinnon, A.J., Patel, P.K., Pretzler, G., Romagnani, L., Schiavi, A., Toncian, T., Willi, O.: High-intensity laser-plasma interaction studies employing laser-driven proton probes. *Laser Part. Beams* **23**, 291 (2005); <https://doi.org/10.1017/S0263034605050408>
- [22] Marburger, J.H., Tooper, R.F.: Nonlinear optical standing waves in overdense plasmas. *Phys. Rev. Lett.* **35**, 1001–1004 (1975); <https://doi.org/10.1103/PhysRevLett.35.1001>
- [23] Bulanov, S.V., Inovenkov, I.N., Kirsanov, V.I., Naumova, N.M., Sakharov, A.S.: Nonlinear depletion of ultrashort and relativistically strong laser pulses in an underdense plasma. *Phys. Fluids B* **4**, 1935–1942 (1992); <https://doi.org/10.1063/1.860046>
- [24] Bulanov, S.V., Esirkepov, T.Z., Naumova, N.M., Pegoraro, F., Vshivkov, V.A.: Solitonlike electromagnetic waves behind a superintense laser pulse in a plasma. *Phys. Rev. Lett.* **82**, 3440–3443 (1999); <https://doi.org/10.1103/PhysRevLett.82.3440>
- [25] Sentoku, Y., Esirkepov, T.Zh., Mima, K., Nishihara, K., Califano, F., Pegoraro, F., Sakagami, H., Kitagawa, Y., Naumova, N.M. Bulanov, S.V.: Bursts of superreflected laser light from inhomogeneous plasmas due to the generation of relativistic solitary waves. *Phys. Rev. Lett.* **83**, 3434 (1999); <https://doi.org/10.1103/PhysRevLett.83.3434>
- [26] Bulanov, S.V., Califano, F., Esirkepov, T.Zh., Mima, K., Naumova, N.M., Nishihara K., Pegoraro, F., Sentoku, Y., Vshivkov, V.A.: Generation of subcycle relativistic solitons by super intense laser pulses in plasmas. *Physica D* **152-153**, 682 (2001); [https://doi.org/10.1016/S0167-2789\(01\)00201-9](https://doi.org/10.1016/S0167-2789(01)00201-9)
- [27] Naumova, N.M., Bulanov, S.V., Esirkepov, T.Z., Farina, D., Nishihara, K., Pegoraro, F., Ruhl, H., Sakharov, A.S.: Formation of electromagnetic postsolitons in plasmas. *Phys. Rev. Lett.* **87**, 185004 (2001); <https://doi.org/10.1103/PhysRevLett.87.185004>
- [28] Esirkepov, T., Nishihara, K., Bulanov, S.V., Pegoraro, F.: Three-dimensional relativistic electromagnetic subcycle solitons. *Phys. Rev. Lett.* **89**, 275002 (2002); <https://doi.org/10.1103/PhysRevLett.89.275002>
- [29] Bulanov, S.S., Esirkepov, T.Z., Kamenets, F.f., Pegoraro, F.: Single-cycle high-intensity electromagnetic pulse generation in the interaction of a plasma wakefield with regular nonlinear structures. *Phys. Rev. E* **73**, 036408 (2006); <https://doi.org/10.1103/PhysRevE.73.036408>
- [30] Wu, D., Zheng, C.Y., Yan, X.Q., Yu, M.Y., He, X.T.: Breather-like penetration of ultrashort linearly polarized laser into over-dense plasmas. *Phys. Plasmas* **20**, 033101

- (2013); <https://doi.org/10.1063/1.4794197>
- [31] Feng, W., Li, J. Q., Kishimoto, Y.: Laser propagation and soliton generation in strongly magnetized plasmas. *Phys. Plasmas* **23**, 032102 (2016); <http://dx.doi.org/10.1063/1.4942789>
- [32] Borghesi, M., Bulanov, S., Campbell, D.H., Clarke, R.J., Esirkepov, T.J., Galimberti, M., Gizzi, L.A., MacKinnon, A.J., Naumova, N.M., Pegoraro, F., Ruhl, H., Schiavi, A., Willi, O.: Macroscopic evidence of soliton formation in multiterawatt laser-plasma interaction. *Phys. Rev. Lett.* **88**, 135002 (2002); <https://doi.org/10.1103/PhysRevLett.88.135002>
- [33] Romagnani, L., Bigongiari, A., Kar, S., Bulanov, S.V., Cecchetti, C.A., Esirkepov, T.Z., Galimberti, M., Jung, R., Liseykina, T.V., Macchi, A., Osterholz, J., Pegoraro, F., Willi, O., Borghesi, M.: Observation of magnetized soliton remnants in the wake of intense laser pulse propagation through plasmas. *Phys. Rev. Lett.* **105**, 175002 (2010); <https://doi.org/10.1103/PhysRevLett.105.175002>
- [34] Sarri, G., Singh, D.K., Davies, J.R., Fiuza, F., Lancaster, K.L., Clark, E.L., Hassan, S., Jiang, J., Kageiwa, N., Lopes, N., Rehman, A., Russo, C., Scott, R.H.H., Tanimoto, T., Najmudin, Z., Tanaka, K.A., Tatarakis, M., Borghesi, M., Norreys, P.A.: Observation of post-soliton expansion following laser propagation through an underdense plasma. *Phys. Rev. Lett.* **105**, 175007 (2010); <https://doi.org/10.1103/PhysRevLett.105.175007>
- [35] Sarri, G., Kar, S., Romagnani, L., Bulanov, S.V., Cecchetti, C.A., Galimberti, M., Gizzi, L.A., Heathcote, R., Jung, R., Kourakis, I., Osterholz, J., Schiavi, A., Willi, O., Borghesi, M.: Observation of plasma density dependence of electromagnetic soliton excitation by an intense laser pulse. *Phys. Plasmas* **18**, 080704 (2011); <https://doi.org/10.1063/1.3625261>
- [36] Chen, L.M., Kotaki, H., Nakajima, K., Koga, J., Bulanov, S.V., Tajima, T., Gu, Y.Q., Peng, H.S., Wang, X.X., Wen, T.S., Liu, H.J., Jiao, C.Y., Zhang, C.G., Huang, X.J., Guo, Y., Zhou, K.N., Hua, J.F., An, W.M., Tang, C.X., Lin, Y.Z.: Self-guiding of 100 TW femtosecond laser pulses in centimeter-scale underdense plasma. *Phys. Plasmas* **14**, 040703 (2007); <https://doi.org/10.1063/1.2720374>
- [37] Pirozhkov, A.S., Ma, J., Kando, M., Esirkepov, T.Z., Fukuda, Y., Chen, L.-M., Daito, I., Ogura, K., Homma, T., Hayashi, Y., Kotaki, H., Sagisaka, A., Mori, M., Koga, J.K., Kawachi, T., Daido, H., Bulanov, S.V., Kimura, T., Kato, Y., Tajima, T.: Frequency multiplication of light back-reflected from a relativistic wake wave. *Phys. Plasmas* **14**, 123106 (2007); <https://doi.org/10.1063/1.2816443>
- [38] Sylla, F., Flacco, A., Kahaly, S., Veltcheva, M., Lifschitz, A., Sanchez-Arriaga, G., Lefebvre, E., Malka, V.: Anticorrelation between ion acceleration and nonlinear coherent structures from laser-underdense plasma interaction. *Phys. Rev. Lett.* **108**, 115003 (2012); <https://doi.org/10.1103/PhysRevLett.108.115003>
- [39] Trines, R. M. G. M., Robinson, A. P. L., Nazarov, W., Kumar, G. R., Pasley, J.: Formation and evolution of post-solitons following a high intensity laser-plasma interaction with a low-density foam target. *Plasma Phys. Control. Fusion* **63** 074001 (2021); <https://doi.org/10.1088/1361-6587/abf85c>
- [40] Sen, A., Kaw, P.K.: Nonlinear 1D laser pulse solitons for particle acceleration. *Phys. Scr.* **T50**, 47 (1994); <https://dx.doi.org/10.1088/0031-8949/1994/T50/007>
- [41] Mima, K., Ohsuga, T., Takabe, H., Nishihara, K., Tajima, T., Zaidman, E., Horton, W.: Wakeless triple-soliton accelerator. *Phys. Rev. Lett.* **57**, 1421 (1986); <https://doi.org/10.1103/PhysRevLett.57.1421>
- [42] Farina, D., Bulanov, S.V.: Relativistic electromagnetic solitons in the electron-ion plasma. *Phys. Rev. Lett.* **86**, 5289–5292 (2001); <https://doi.org/10.1103/PhysRevLett.86.5289>
- [43] Kuehl, H.H., Zhang, C.Y.: One-dimensional, weakly nonlinear electromagnetic solitary waves in a plasma. *Phys. Rev. E* **48**, 1316 (1993); <https://doi.org/10.1103/PhysRevE.48.1316>
- [44] Farina, D., Bulanov, S.V.: Dynamics of relativistic solitons. *Plasma Phys. Control. Fusion* **47**, A73 (2005); <https://dx.doi.org/10.1088/0741-3335/47/5A/007>; Farina, D., Bulanov, S.V.: Slow electromagnetic solitons in electron-ion plasmas. *Plasma Phys. Rep.* **27**, 641–651 (2001); <https://doi.org/10.1134/1.1390536>
- [45] Poornakala, S., Das, A., Kaw, P.K., Sen, A., Sheng, Z.M., Sentoku, Y., Mima, K., Nishikawa, K.: Weakly relativistic one-dimensional laser pulse envelope solitons in a warm plasma. *Phys. Plasmas* **9**, 3802–3810 (2002); <https://doi.org/10.1063/1.1496085>
- [46] Saxena, A., Das, A., Sen, A., Kaw, P., Fluid simulation studies of the dynamical behavior of one-dimensional relativistic electromagnetic solitons. *Phys. Plasmas* **13**, 032309 (2006); <https://doi.org/10.1063/1.2187447>
- [47] Lontano, M., Passoni, M., Bulanov, S.V.: Relativistic electromagnetic solitons in a warm quasineutral electron-ion plasma. *Phys. Plasmas* **10**, 639 (2003); <https://doi.org/10.1063/1.1544666> Lontano, M., Bulanov, S.V., Koga, J., Passoni, M., Tajima, T.: A kinetic model for the one-dimensional electromagnetic solitons in an isothermal plasma *Phys. Plasmas* **9**, 2562–2568 (2002); <https://doi.org/10.1063/1.1476307>
- [48] Eliasson, B., Shukla, P.K.: Kinetic effects on relativistic solitons in plasmas. *Phys. Lett. A* **354** (5-6), 453–456 (2006); <https://doi.org/10.1016/j.physleta.2006.01.083>
- [49] Saxena, V., Das, A., Sengupta, S., Kaw, P., Sen, A.: Stability of nonlinear one-dimensional laser pulse solitons in a plasma. *Phys. Plasmas* **14**, 072307 (2007); <https://doi.org/10.1063/1.2749227> Saxena, V., Das, A., Sengupta, S., Kaw, P., Sen, A.: Stability of one-dimensional relativistic laser plasma envelope solitons. *J. Phys.: Conf. Ser.* **112**, 022110 (2008); <https://dx.doi.org/10.1088/1742-6596/112/2/022110>
- [50] Lehmann, G., Laedke, E.W., Spatschek, K.H.: Stability and evolution of one-dimensional relativistic solitons on the ion time scale. *Phys. Plasmas* **13**, 092302 (2006); <https://doi.org/10.1063/1.2338820>
- [51] Pukhov, A., Meyer-ter-Vehn, J.: Relativistic magnetic self-channeling of light in near-critical plasma: Three-dimensional particle-in-cell simulation. *Phys. Rev. Lett.* **76**, 3975–3978 (1996); <https://doi.org/10.1103/PhysRevLett.76.3975>
- [52] Hurricane, O.A., Callahan, D.A., Springer, P.T., Edwards, M.J., Patel, P., Baker, K., Casey, D.T., Divol, L., Döppner, T., Hinkel, D.E., et al. Beyond alpha-heating: Driving inertially confined fusion implosions toward a burning-plasma state on the National Ignition Facility. *Plasma Phys. Control. Fusion*, **61**, 014033. (2018); <https://doi.org/10.1088/1361-6587/aaed71>

- [53] Borghesi, M., MacKinnon, A.L., Bell, A.R., Gaillard, R., Willi, O.: Megagauss magnetic field generation and plasma jet formation on solid targets irradiated by an ultraintense picosecond laser pulse. *Phys. Rev. Lett.* **81**, 112–115 (1998); <https://doi.org/10.1103/PhysRevLett.81.112>
- [54] Briand, J., Adrian, V., Tamer, M.El., Gomes, A., Quemener, Y., Dinguirard, J.P., Kiefferet, J.C.: Axial magnetic fields in laser-produced plasmas. *Phys. Rev. Lett.* **54**, 38 (1985); <https://doi.org/10.1103/PhysRevLett.54.38>
- [55] Tatarakis, M., Gopal, A., Watts, I., Beg, F.N., Dangor, A.E., Krushelnick, K., Wagner, U., Norreys, P.A., Clark, E.L., Zepf, M., Evans, R.G.: Measurements of ultrastrong magnetic fields during relativistic laser–plasma interactions. *Phys. Plasmas* **9**, 2244 (2002); <https://doi.org/10.1063/1.1469027>
- [56] Shukla, P.K., Stenflo, L.: Nonlinear propagation of electromagnetic waves in magnetized plasmas. *Phys. Rev. A* **30**, 2110 (1984); <https://doi.org/10.1103/PhysRevA.30.2110>
- [57] Nagesha Rao, N., Shukla, P.K., Yu, M.Y.: Strong electromagnetic pulses in magnetized plasmas. *Phys. Fluids* **27**, 2664–2668 (1984); <https://doi.org/10.1063/1.864568>
- [58] Rao, N.N.: Theory of near-sonic envelope electromagnetic waves in magnetized plasmas. *Phys. Rev. A* **37**, 4846–4853 (1988); <https://doi.org/10.1103/PhysRevA.37.4846>
- [59] Farina, D., Lontano, M., Bulanov, S.: Relativistic solitons in magnetized plasmas. *Phys. Rev. E* **62**, 4146–(2000); <https://doi.org/10.1103/PhysRevE.62.4146>
- [60] Jeffrey, A., Kawahara, T.: *Asymptotic Methods in Nonlinear Wave Theory*. Pitman, Boston (1982)
- [61] Kourakis, I., Shukla, P.K.: Exact theory for localized envelope modulated electrostatic wavepackets in space and dusty plasmas. *Nonlinear Process. Geophys.* **12**, 407–423 (2005); <https://doi.org/10.5194/npg-12-407-2005>
- [62] Veldes, G.P., Borhanian, J., McKerr, M., Saxena, V., Frantzeskakis, D.J., Kourakis, I.: Electromagnetic rogue waves in beam-plasma interactions. *J. Opt.* **15** (6), 064003 (2013); <https://dx.doi.org/10.1088/2040-8978/15/6/064003>
- [63] Segre, S.E.: A review of plasma polarimetry - theory and methods. *Plasma Phys. Control. Fusion* **41**, R57 (1999); <https://dx.doi.org/10.1088/0741-3335/41/2/001>
- [64] Taniuti, T., Yajima, Y.: Perturbation Method for a Nonlinear Wave Modulation. I. *J. Math. Phys.* **10**, 1369–1372 (1969); <https://doi.org/10.1063/1.1664975>; Asano, N., Taniuti, T., Yajima, N.: Perturbation Method for a Nonlinear Wave Modulation. II. *ibid.* **10**, 2020–2024 (1969); <https://doi.org/10.1063/1.1664797>
- [65] Swanson, D.G.: *Plasma Waves*, Academic Press, INC, San Diego (1989)
- [66] Remoissenet, M.: *Waves Called Solitons*. Springer-Verlag, Berlin, 2nd Ed. (1996)
- [67] Dauxois, T., Peyrard, M.: *Physics of Solitons*. Cambridge University Press, Cambridge (2006)
- [68] Fedele, R., Schamel, H.: Solitary waves in the Madelung’s fluid: Connection between the nonlinear Schrödinger equation and the Korteweg-de Vries equation. *Eur. Phys. J. B* **27**, 313–320 (2002); <https://doi.org/10.1140/epjb/e2002-00160-7>; Fedele, R.: Envelope solitons versus solitons. *Phys. Scr.* **65**, 502 (2002); <https://dx.doi.org/10.1238/Physica.Regular.065a00502>
- [69] Borhanian, J., Sobhanian, S., Kourakis, I., Esfandyari-Kalejahi, A.: Evolution of linearly polarized electromagnetic pulses in laser plasmas. *Phys. Plasmas* **15**, 093108 (2008); <https://doi.org/10.1063/1.2990023>
- [70] Kivshar, Yu.S., Agrawal, G.P.: *Optical solitons: from fibers to photonic crystals*. Academic Press, San Diego (2003)
- [71] Veldes, G.P., Cuevas, J., Kevrekidis, P.G., Frantzeskakis, D.J.: Coupled backward- and forward-propagating solitons in a composite right- and left-handed transmission line. *Phys. Rev. E* **88**, 013203 (2013); <https://doi.org/10.1103/PhysRevE.88.013203>
- [72] Kourakis, I., Shukla, P.K., Morfill, G.: Modulational instability and localized excitations involving two nonlinearly coupled upper-hybrid waves in plasmas. *New J. Phys.* **7**, 153 (2005); <https://dx.doi.org/10.1088/1367-2630/7/1/153>
- [73] Lazarides, N., Veldes, G.P., Javed, A., Kourakis, I.: Modulational electrostatic wave-wave interactions in plasma fluids modeled by asymmetric coupled nonlinear Schrödinger (CNLS) equations. *Chaos, Solitons and Fractals* **175**, 113974 (2023); <https://doi.org/10.1016/j.chaos.2023.113974>
- [74] Lazarides, N., Kourakis, I.: Coupled nonlinear Schrödinger (CNLS) equations for two interacting electrostatic wavepackets in a non-Maxwellian fluid plasma model. *Nonlinear Dyn.* **112**, 2795–2819 (2024). <https://doi.org/10.1007/s11071-023-09165-4>
- [75] Lazarides, N., Veldes, G.P., Frantzeskakis, D.J., Kourakis, I.: Electrostatic wave interaction via asymmetric vector solitons as precursor to rogue wave formation in non-Maxwellian plasmas. *Sci. Rep.* **14**, 2150 (2024). <https://doi.org/10.1038/s41598-024-52431-7>

## VII. DECLARATIONS

### A. Funding

Authors IK and NL gratefully acknowledge financial support from Khalifa University of Science and Technology, Abu Dhabi, United Arab Emirates, via the project CIRA-2021-064 (8474000412) (PI Ioannis Kourakis). IK also acknowledges financial support from KU via the project FSU-2021-012 (8474000352) (PI Ioannis Kourakis) as well as from KU Space and Planetary Science Center, via grant No. KU-SPSC-8474000336 (PI Mohamed Ramy Mohamed Elmaarry).

### B. Competing Interests

The authors have no relevant financial or non-financial interests to disclose.

### C. Author Contributions

G. P. Veldes carried out the algebraic work, contributed to the methodology, software development,



and numerical analysis. N. Lazarides contributed to the methodology and reviewed the manuscript. D. J. Frantzeskakis contributed to the concept and design, and reviewed the manuscript. I. Kourakis contributed to the problem conception, project design, launch and methodology, reviewed the manuscript, and managed project funding. All authors read and approved the final manuscript.

#### **D. Data Availability**

The datasets generated during and/or analysed during the current study are available from the corresponding author on reasonable request.